Non-Bloch plasmonic stop-band in real-metal gratings

Evgeny Popov, Nicolas Bonod, Stefan Enoch

Institut Fresnel, CNRS UMR6133,Université de Provence,
Domaine universitaire de St Jérôme, 13397 MARSEILLE Cedex 20, France

Recent studies of plasmon surface wave (PSW) propagation in short-period perfectly conducting gratings have shown formation of stop-band that are not linked to the interaction between two (counter) propagating surface waves. We study the properties of this stop-band in real metals. While for both perfectly conducting and real metals the propagation constant of PSW grows with the groove height, the stop-band in real metals appears for groove heights significantly smaller than in perfect metals. A physical explanation of the formation of the stop-band is proposed both by using a homogenisation of the corrugated layer and by analysis of the tangential electric field component.

©2007 Optical Society of America

OCIS codes: (240.6680) Surface plasmons; (050.1950) Diffraction gratings

---

References and links

1. F. J. Garcia-Vidal, L. Martin-Moreno, and J. B. Pendry, "Surfaces with holes in them: new plasmonic metamaterials," J. Opt. A: Pure Appl. Opt. **7**, S97-S101 (2005).
2. J. B. Pendry, L. Martin-Moreno, and F. J. Garcia-Vidal, "Mimicking surface plasmons with structured surfaces," Science **305**, 847-848 (2004).
3. R. W. Wood: "On a remarkable case of uneven distribution of light in a diffraction grating spectrum," Phylos. Mag. **4**, 396-402 (1902).
4. D. Maystre, "General study of grating anomalies from electromagnetic surface modes," in *Electromagnetic Surface Modes*, A. D. Boardman, ed., (John Wiley, 1982), ch.17.
5. E. Popov, "Light diffraction by relief gratings: a microscopic and macroscopic view," in *Progress in Optics*, E.Wolf, ed., (Elsevier, Amsterdam, 1993) Vol. **31**, pp. 139–187.
6. E. Popov, L. Tsonev, and D. Maystre, "Losses of plasmon surface wave on metallic grating," J. Mod. Opt. **37**, 379-387 (1990).
7. F. J. Garcia-Vidal, J. Sánchez-Dehesa, A. Dechelette, E. Bustarret, T. López-Rios, T. Fournier, and B. Pannetier, "Localized surface plasmons in lamellar metallic gratings," J. Lightwave Technol. **17**, 2191-2195 (1999).
8. W.-C. Tan, T. W. Preist, J. R. Sambles, and N. P. Wanstall, "Flat surface-plasmon-polariton bands and resonant optical absorption on short-pitch metal gratings," Phys. Rev. B **59**, 12661 (1999).
9. I. R. Hooper and J. R. Sambles, "Surface plasmon polaritons on narrow-ridged short-pitch metal gratings," Phys. Rev. B **66**, 205408 (2002).
10. I. R. Hooper and J. R. Sambles, "Dispersion of surface plasmon polaritons on short-pitch metal gratings," Phys. Rev. B **65**, 165432-1 – 9 (2002).
11. S. Maier, S. Andrews, L. Martin-Moreno, and F. J. Garcia-Vidal, "Terahertz surface plasmon-polariton propagation and focusing on periodically corrugated metal wires," Phys. Rev. Lett. **97**, 176805-1 – 4 (2006).
12. J. D. Jackson, *Classical Electrodynamics* (Wiley, 1998), sec. 8.5.
13. E. Popov, M. Nevière, J. Wenger, P.-F. Lenne , H. Rigneault, P. Chaumet, N. Bonod, J. Dintinger, and T. Ebbesen, "Field enhancement in single subwavelength apertures," J. Opt. Soc. Am. A **23**, 2342-2348 (2006).
14. R. McPhedran, L. Boten, M. Craig, M. Nevière, and D. Maystre, "Lossy lamellar gratings in the quasistatic limit," Opt. Acta **29**, 289-312 (1982).
15. G. Bouchitte and R. Petit, "Homogenization techniques as applied in the electromagnetic theory of gratings," Electromagnetics **5**, 17-36 (1985).
16. P. Yeh, "A new optical model for wire grid polarizers," Opt. Commun. **26**, 289-292 (1978).
17. E. Popov and M. Nevière: "Maxwell equations in Fourier space: fast converging formulation for diffraction by arbitrary shaped, periodic, anisotropic media," J. Opt. Soc. Am. A **17**, 1773 (2001).

18. M. G. Moharam and T. K. Gaylord, "Rigorous coupled-wave analysis of dielectric surface-relief gratings," J. Opt. Soc. Am. **72**, 1385-1392 (1982)
19. P. Lalanne and G. M. Morris, "Highly improved convergence of the coupled-wave method for TM polarization," J. Opt. Soc. Am. A **13**, 779-784 (1996)
20. G. Granet and B. Guizal, "Efficient implementation of the coupled-wave method for metallic gratings in TM polarization," J. Opt. Soc. Am. A **13**, 1019-1023 (1996)
21. E. Popov, L. Tsonev, and D. Maystre, "Losses of plasmon surface wave on metallic grating," J. Mod. Opt. **37**, 379-387 (1990)

Introduction

Stop-bands in periodic media are usually due to interaction between different eigenmodes, an interaction which modifies modal dispersion curves close to their intersection points. Recently [1], it has been demonstrated that another type of stop-band can appear in short-period gratings made of infinitely conducting metal, creating conditions of existence for plasmon-like surface wave. The explanation of this phenomenon was found in the interaction between the surface states and the modes propagating inside the grooves [2]. Our aim is to extend the study to real metals, and to show significant differences between real and perfect metals. When considering real metals, considerable activity has been observed since the start of the 20th century [3] and, in particular during the last 25 years. An interested reader can find an early review by Maystre [4] and later by Popov [5] on the role of plasmon excitation on shallow and deep [6] metallic gratings, a topic of increasing interest during the last 10 years [7-11].

Our aim is to extend the work made in [1] to real-metal gratings in order to investigate the similarities and the differences from the perfectly conducting case. In particular, the stop band for real metals appears for groove height values significantly smaller than for perfectly conducting metals. The other difference is that, contrary to perfect metals, the stop-band height for real metals decreases with the grating period. An increase of the propagation constant of the surface mode with the groove height is observed in both cases. We give physical insight thanks to homogenization of the corrugated layer and observation of field maps.

First section is devoted to stop bands for perfectly conducting gratings. The position of the stop band as a function of the period and the groove height of the grating is studied, to be followed in the second section by a similar study for the real-metal case, namely for aluminium in visible. Stop bands are also observed, but emphasis is then made on the difference with the perfect metal case. Firstly, the stop band appears for smaller groove height. Secondly, the stop band critical value of the groove height h decreases with the grating period d, contrary to the behaviour observed in perfect metals. It has been shown in [1] that in the limit when $d \rightarrow 0$, the modal structure of the equivalent homogenized optically anisotropic layer explains the existence and the dependence of the stop band with the groove height. In perfectly conducting case, the homogenized layer presents anisotropic permittivity and permeability, whereas with real metals, the homogenized layer presents only anisotropic permittivity. It is shown in the third section that this difference explains why the stop band appears for smaller groove heights in real metals. In the fourth section, we present an alternative approach to explain the increase of the propagation constant with the groove height and the formation of the stop band. The approach is based on an analysis of the tangential component (E_x) of the electric field at the top and bottom of the groove, which clearly indicates whether the conditions for the existence of a surface wave are satisfied or not. The tangential component must almost vanish at the surface of a highly conducting metal, a condition satisfied on the lamellae tops and at the groove bottoms. However, as the groove depth varies, the values of E_x at the groove openings becomes significantly non-vanishing, which perturbs the propagation of the surface wave, reduces its velocity (i.e. increases its propagation constant) and, under certain conditions can lead to a complete cut-off of the surface wave.

Stop bands in corrugated perfectly conducting metals

Plasmon-like surface wave can propagate on the surface of a corrugated perfectly conducting metal. Periodic perturbation of the surface (having a period d) can couple the counter propagating modes, modifying their propagation constants (denoted as k_x) in the regions close to the boundaries of the Brillouin zone. The results presented in this section are already known, but they are necessary for making the comparison with the real-metal case.
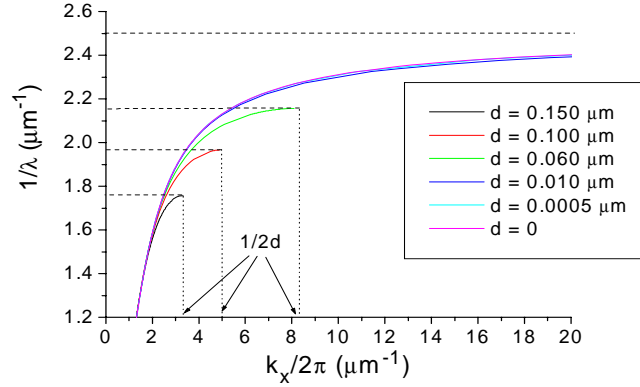

Fig. 1. Dispersion curves of plasmon-like surface waves in a lamellar grating made of perfectly conducting metal. Dotted lines present Brillouin zone boundaries ($k_x = \pi/d$), dashed lines indicate lower boundary of the forbidden zone created by the interaction between counter propagating surface waves.

Figure 1 presents the dispersion curves in the case of lamellar metallic gratings for several values of the grating period d. The period d and the incident wavelength λ are in μm. The dotted lines indicate the Brillouin zone boundaries:

$$k_{x,max} = \frac{\pi}{d} \qquad (1)$$

and the dashed lines indicate the lower boundary of the forbidden zone created by the interaction between the counter-propagating waves. For very small groove depth values (weak counter-propagating interaction), the two boundaries are linked through the free-space relation:

$$\omega_{max}/c = k_{x,max}, \quad h \to 0 \qquad (2)$$

These boundaries increase with the period reduction, as observed in Fig. 1. It can be expected from Eq. (2) that ω_{max} grows to infinity when d is reduced. However, as shown in [1], there is an upper limit reached asymptotically when $d \to 0$, a limit which depends on the groove depth h through the simple relation $\lambda = 4h$, as shown by the blue line in Fig. 2.

Surface wave propagation constant k_x increases from the free-space value $k_0 = 2\pi/\lambda$ with the increase of the groove depth (Fig. 2), due to the stronger counter-propagating modal interaction. As observed in Fig. 2, this difference $k_x - k_0$ for a fixed wavelength and groove depth values is smaller for shorter periods, because the shorter the period the farther the Brillouin zone boundary. However, as already observed in Fig. 1, a stop-band is formed in Fig. 2 in the h-space for $h > \lambda/4$, even when $d \to 0$.

This phenomenon finds its explanation in the modal structure of the equivalent waveguide formed inside the corrugated layer, a waveguide having anisotropic optical

constants [1, 2]. In the next sections, we detail this homogenization approach for both real and perfectly conducting metals, and point out their differences.
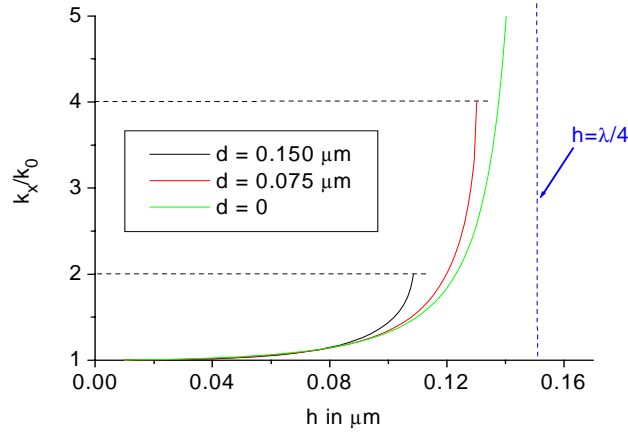

Fig. 2. Normalized propagation constant of the plasmon-like surface wave as a function of the groove height of the grating for 3 values of the period and wavelength λ = 0.6 µm. In the limit d→0, the cut-off height is equal to λ/4.

Stop bands in real metals

Plasmon surface wave along real-metal grating has absorption losses, and Fig. 3 represents the real and imaginary part of the propagation constant of the eigenmode k_x as a function of the groove height in the case of an aluminium grating illuminated in the visible (wavelength λ = 0.6 µm and refractive index n = 1.378 + i 7.616). Qualitatively, the effect is similar to that one observed in Fig. 2, but several important differences must be evidenced. First, close to the cut-off, the imaginary part of the plasmon propagation constant starts to grow rapidly, accompanied by a maximum of its real part. This behavior is quite typical to the modes of lossy systems close to their cut-off [12, 13].
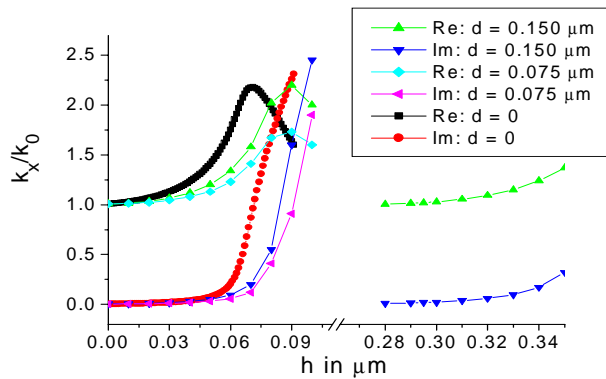

Fig. 3. Same as in Fig. 2 but for a real metal (aluminum in visible). Cut-off is characterized by the sharp increase of the imaginary part of the propagation constant. As for perfect metals, the real part of k_x increases at the cut-off.

Second, the decrease of the period for real metal case (Fig. 3) moves the cut-off towards smaller groove depth values, contrary to the perfectly conducting case (Fig. 2). Third, although contrary to perfectly conducting metal in Figs. 1 and 2, the position of the cut-off is

not quite well defined, its values for real metals are much lower than for the perfectly conducting case. Whether this is due to the penetration of the electromagnetic field inside the substrate, which increases the visible groove depth, is a question that can partially explain this difference, by taking into account that the skin depth is approximately equal to 12 nm. However, this reason does not provide a complete explanation, as shown in Fig. 4, where the PSW propagating constants are presented as a function of the groove depth for a very short-period grating (d = 0.0015 µm) having aluminium lamellae and, respectively, aluminium or perfectly conducting substrates. As observed, even in the case of perfectly conducting substrate and lossy lamellae, the cut-off height is almost twice smaller than in Fig. 2.
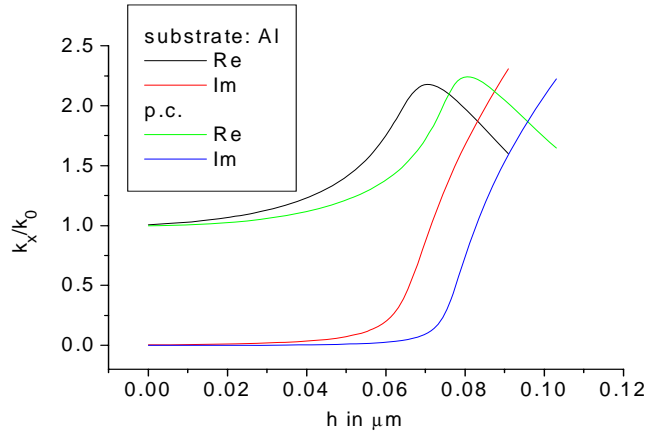

Fig. 4. Same as in Figs. 2 and 3 but for two different gratings. Lamellae and substrate made of aluminum (black and red lines), and lamellae made of aluminum and substrate made of perfect metal (green and blue lines). Wavelength $\lambda = 0.6$ µm.

Homogenized corrugated layer for perfect and real metals

As discussed in detail in [1], the perfectly conducting lamellar grating behaves, in the limit of $d \to 0$ as an anisotropic waveguide with both relative permittivity and relative permeability being tensors:

$$\varepsilon_{xx} = \left\langle \frac{1}{\varepsilon} \right\rangle^{-1}, \varepsilon_{yy} = \varepsilon_{zz} = \infty \qquad (3)$$

$$\mu_{xx} = 1, \mu_{yy} = \mu_{zz} = 1/\varepsilon_{xx} \qquad (4)$$

where the angular brackets stay for the mean value. When $d \to 0$, both the spectral and the groove-depth dependency, as presented in Figs. 1 and 2, approach the characteristics of a planar anisotropic waveguide. While the anisotropic homogenized tensor <ε> is quite well known since long time [14, 15], the anisotropic homogenized tensor <μ> depicted by Eq. (2) is necessary only for perfectly conducting lamellae in order to ensure that the electromagnetic waves travelling inside the grooves in direction of either y and z have, correspondingly, the wavevector components equal to $k_y / k_0 = 1$ and $k_z / k_0 = 1$. This is due to the fact that for small groove width, the only propagating mode inside the grooves is the fundamental TEM mode. And indeed, when observing the black curve in Fig. 5, which gives the vertical distribution of $|E_x|$ inside the groove for an almost infinitely conducting material (made with $\varepsilon_{metal} = -10^4 + i\ 10^7$, corresponding to Al in the microwave domain), one observes that $|E_x|$ reaches from a minimum at the groove bottom to a maximum at the groove opening at a distance along the y-axis exactly equal to a quarter-wavelength. This result shows that the

component k_y of the fundamental mode inside the groove (which determines the y-dependence of the field) is equal to the free space constant k_0, *i.e.* $k_y = k_0$.
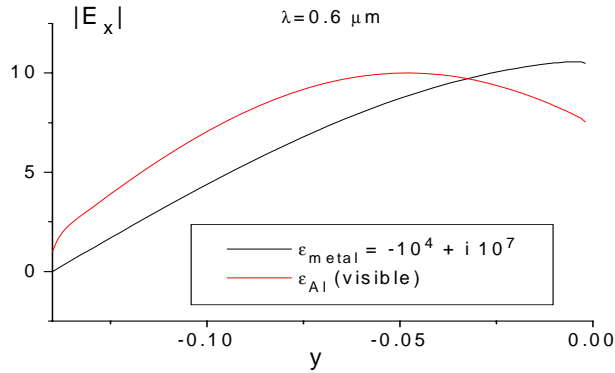

Fig. 5. Vertical distribution of $|E_x|$ inside the groove with depth $h = 0.13$ µm for a perfect (black line) and real-metal (red line) case. Incident electric field modulus is equal to 1.

On the other hand, finitely conducting gratings have equivalent homogenized presentation, which represents a waveguide, anisotropic in its dielectric permittivity whereas its magnetic permeability is isotropic:

$$\varepsilon_{xx} = \left\langle \frac{1}{\varepsilon} \right\rangle^{-1}, \varepsilon_{yy} = \varepsilon_{zz} = \langle \varepsilon \rangle, \tag{5}$$

$$\mu_{xx} = \mu_{yy} = \mu_{zz} = 1, \tag{6}$$

And indeed, numerical results show that when $d \to 0$, the curves presented in Fig. 3 for $d \neq 0$ tend towards the curve for an anisotropic waveguide with permittivity given by Eq. (5) similar to Eq. (3), but with isotropic permeability presented by Eq. (6). The discontinuity in the transition between highly but finitely conducting metals to a perfectly conducting material in the homogenization procedure is known since more than 20 years [14-16] and is still waiting for a satisfactory explanation. Anyway, the main difference is that in the case of a finite conductivity, the propagation constant in y-direction inside the homogenized anisotropic waveguide becomes different from k_0:

$$k_y / k_0 = \left\langle \frac{1}{\varepsilon} \right\rangle^{-1/2}. \tag{7}$$

If we consider a highly conducting grating with filling ratio of 0.5, then $k_y / k_0 = \sqrt{2}$, i.e., the electromagnetic field components vary inside the equivalent anisotropic waveguide more rapidly than for perfect metals. This can be observed in Fig. 5, where the second curve is for a grating made of Al illuminated in the visible. This more rapid variation explains why the surface wave cut-off appears at shallower grooves for lossy gratings when compared to lossless material. The increase of the mode propagation constant with the groove depth can be understood from the analogy with an equivalent waveguide. Plasmon-like surface wave in real but highly conducting metals is characterized by a propagation constant almost equal to the free-space wavenumber, with a slightly greater real part and small positive imaginary part. When a dielectric layer with $\varepsilon_x = 1/\langle 1/\varepsilon \rangle$ (≈ 2 for filling ratio of 0.5) is deposited on the metallic surface, the propagation constant of the PSW increases its values, the increase being larger when the layer thickness grows up. Moreover, unlike the isotropic waveguide, the anisotropic waveguide has an upper cut-off thickness, which explains the PSW cut-off observed in Figs. 2 and 3.

These numerical results are obtained using the differential theory of gratings [17] in its rigorous coupled-wave version [18-20]. The method is based on a projection of Maxwell equations of a Fourier basis and thus reducing them to a set of ordinary differential equations, by playing special attention to the factorization rules used in a truncated basis of functions [19, 20]. In the case of lamellar groove profile, the set of equations is solved using eigenvalue-eigenvector technique [18], which increases significantly the computation speed. The numerical results are supported by analytical analysis of the guided wave propagation in an anisotropic waveguide, made in the Appendix. The result, described by Eq. (15) in the case of highly (or perfectly, as discussed in Ref. [1]) conducting substrate and lamellae confirm the behavior of the mode propagating constant k_x, presented in Figs. 2 and 3. With the increase of the groove depth, k_x increases as $tg(k_{y,2}h)$, i.e., there is a cut-off situated at $h = \pi/2k_{y,2}$. This formula explains, as well, the difference between the perfectly conducting and real-metal case, when taking into account the couples of Eqs. (3) and (4) or (5) and (6):

$$h_{cut} = \frac{\pi}{2k_{y,2}} = \frac{\lambda}{4\sqrt{\mu_{zz}\varepsilon_{xx}}} = \begin{cases} \dfrac{\lambda}{4}, & p.c \\ \dfrac{\lambda}{4}\sqrt{f}, & f.c \end{cases} \tag{8}$$

where p.c. and f.c. stand for perfect or finite conductivity and f is the ratio between the groove width and period.

In addition, Eq. (15) contains a second (or higher) branch of the surface plasmon, existing in deep gratings ($h \sim \lambda/2$), shown in the right-hand side of Fig. 3 and discussed in detail in Ref. [7] for lamellar grooves and in Ref. [21] for sinusoidal gratings.

Local field analysis

As expected for highly conducting metals, the PSW wave has an almost vanishing electric field component E_x tangential to the metal surface. When a surface corrugation is introduced, the same condition is fulfilled on both the lamella top and the groove bottom.
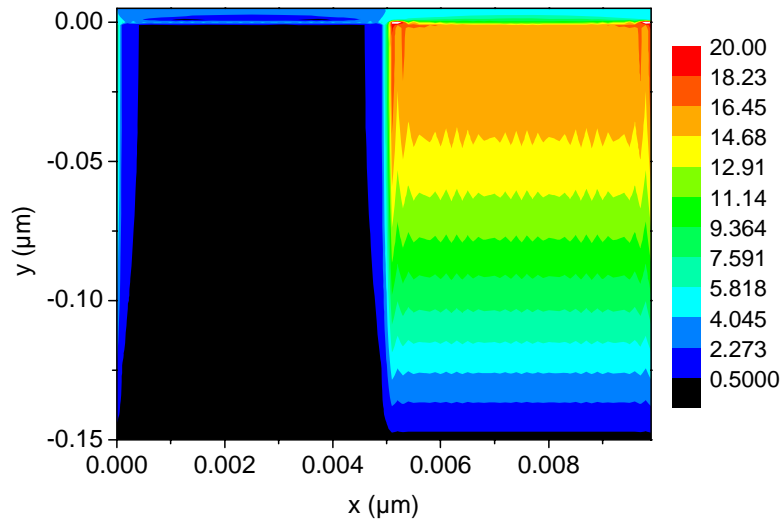

Fig. 6. Map of $|E_x|$ within one period of the grating with $h = \lambda/4$. Wavelength $\lambda = 0.6$ µm, period $d = 0.01$ µm, and $\varepsilon_{metal} = -10^4 + i \, 10^7$. $|E_x|$ vanishes on the top of the lamella and at the bottom of the groove, and has a maximum at the groove opening.

When considering a flat surface of a perfect metal, the propagation constant of the surface wave k_x is equal to k_0, and the tangential component of the electric field E_x is null. With the presence of a grating, the electric field component E_x is not null at the surface of the vertical walls, because it represents the normal component to the wall (E_y is then null). As a consequence, the propagation constant of the surface mode must be different from k_0 (otherwise $E_x \equiv 0$ everywhere), and only the condition $k_x > k_0$ corresponds to a surface wave. This analysis explains why, if the PSW exists on a corrugated surface, its propagating constant is greater than for the wave on a flat surface.

In addition, when going up from the metal surface into the cover (vacuum or dielectric), $|E_x|$ increases (at least up to a given height), because $k_x \neq k_0$. Thus even for very shallow grooves, the condition:

$$E_x \approx 0 \ \text{at} \ y = 0, \tag{9}$$

i.e. on the straight line lying on the lamella surface is not fulfilled over the groove openings, while still holding on the lamellae tops. Thus the condition (9) necessary for the 'ideal' surface wave propagation along a highly conducting metal-dielectric interface is perturbed, as shown in Fig. 6, a perturbation resulting in slowing down the plasmon, i.e. in increasing its propagation constant k_x.
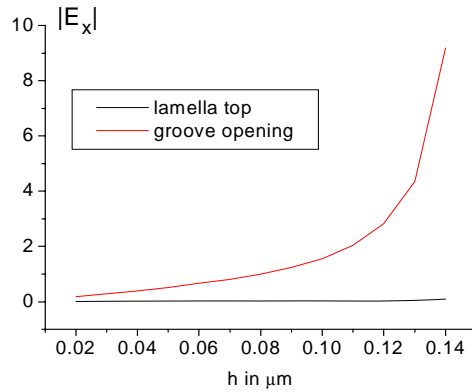

Fig. 7. Comparison of the values of $|E_x|$ at the top of the lamellae (black line) and at the groove opening (red line) as a function of the height of the groove. $\lambda = 0.6$ µm, d = 0.01 µm, and aluminium in the microwave domain, $\varepsilon_{metal} = -10^4 + i \, 10^7$.

The perturbation grows with the groove depth, as observed in Fig. 7, which shows the values of $|E_x|$ on the lamellae top and in the middle of the groove opening for different groove depths of a very short-period lamellar grating ($\lambda/d = 60$) made of very highly conducting material. It is observed that $|E_x|$ (normalized so that $|E| = 1$) exhibits a sharp jump from lamellae top to groove opening, a jump which grows with h and perturbs the propagation of the plasmon surface waves thus reducing its speed for deeper grooves.

The fundamental TEM mode inside the grooves forms a standing wave with a period equal to $\lambda/2$. When the groove depth approaches a quarter-wavelength, $|E_x|$ reaches a maximum at the groove openings (see Fig. 7) and the surface plasmon is so perturbed that it cannot propagate (its velocity becomes zero and its propagation constant tends toward infinity), i.e., the mode is cut-off.

Similar is the behavior when lossy grating material is considered. The difference lies in the fact that when k_x increases (i.e., when the plasmon velocity diminishes), the absorption losses increase [3]. This phenomenon has already been observed in Fig. 3 with the sharp increase of the imaginary part of the propagation constant close to the cut-off, i.e., when the $|E_x|$ component at the top of the groove is maximum. A second difference lies in the fact that

in lossy metals, the propagation constant of the fundamental mode inside the groove is larger than k_0. As a consequence, the variation in y-direction of the electric field components is faster than for perfectly conducting gratings. Thus when increasing the groove height, $|E_x|$ will reach its maximum value at a groove height h smaller than $\lambda/4$.

Conclusion

It is shown that gratings with very short period made of real metals support plasmon-like surface wave in the same way as it has been recently shown with perfect metals. These surface wave present a cut-off groove height value. A thorough comparison between perfect and real metals has been carried out and important differences have been pointed out. First, for real metals, the cut-off height diminishes with the period d, while for perfectly conducting gratings the tendency is the opposite. Second, the cut-off height is smaller for real metals. Third, with real metals, the cut-off is accompanied by a sharp increase of the imaginary part of the propagation constant. In all cases, the propagation constant increases with the groove height. We present two approaches to explain these phenomenon. The first one is based on the homogenization of the corrugated layer, as it has been proposed in Refs. [1, 2] for perfectly conducting gratings. In both cases (real and perfect metals), the equivalent homogenized layer presents an anisotropic dielectric permittivity, which explains why the propagation constant of the surface mode increases with the groove height. On the other hand, the homogenized layer presents an anisotropic magnetic permeability only in the case of perfect metals, a permeability remaining scalar in the real-metal case. This difference explains why the cut-off height is smaller in the latter case, as the variation of the electric field components inside the grooves is more rapid.

Another explanation of these peculiarities is given by analyzing the behavior of the tangential component of the electric field above and inside the grooves of the grating.

Acknowledgements

Appendix

The behavior of the anisotropic waveguide equivalent to the lamellar metallic grating is quite different from the well-known behavior of isotropic dielectric or metallic waveguides. In particular, the anisotropic waveguide is characterized by the existence of an *upper* cut-off thickness, which explains the cut-off of the PSW for larger groove depths, observed in Figs. 3 and 4. Let us consider a waveguide with anisotropic relative permittivity and permittivity:

$$\varepsilon = \begin{pmatrix} \varepsilon_{xx} & 0 & 0 \\ 0 & \varepsilon_{yy} & 0 \\ 0 & 0 & \varepsilon_{zz} \end{pmatrix}, \quad \mu = \begin{pmatrix} \mu_{xx} & 0 & 0 \\ 0 & \mu_{yy} & 0 \\ 0 & 0 & \mu_{zz} \end{pmatrix} \tag{10}$$

It can be easily found from the Maxwell equations that for diagonal form of anisotropy, it is possible to separate the two fundamental case of transverse electric (TE) and magnetic (TM) polarization. The propagation equation for H_z in the TM case is similar to the isotropic case:

$$\frac{d^2 H_z}{dy^2} + \left(k_0^2 \varepsilon_{xx} \mu_{zz} - k_x^2 \frac{\varepsilon_{xx}}{\varepsilon_{yy}} \right) H_z = 0 \tag{11}$$

assuming an $\exp(ik_x x)$ variation. The boundary conditions at the waveguide surfaces lead to the well-known characteristic equation for the mode propagation constant k_x, which has the same form as for isotropic media:

$$(\beta + \alpha)(\beta + \gamma)\exp(-ik_{y,2}h) = (\beta - \alpha)(\beta - \gamma)\exp(ik_{y,2}h) \qquad (12)$$

where $\alpha = k_{1,y}/\varepsilon_1$ characterizes the cladding with relative permittivity ε_1, $\gamma = k_{3,y}/\varepsilon_3$ characterizes the substrate having permittivity ε_3, and $\beta = k_{2,y}/\varepsilon_{xx}$ with

$$k_{y,2} = \sqrt{k_0^2 \varepsilon_{xx}\mu_{zz} - k_x^2 \frac{\varepsilon_{xx}}{\varepsilon_{yy}}} \qquad (13)$$

as found from Eq. (11).

Let us consider highly conducting substrate, so that $\gamma \ll \beta$ and Eq. (12) is simplified to take the form:

$$\alpha = i\beta\, \mathrm{tg}(k_{y,2}h). \qquad (14)$$

For isotropic waveguides, both α and β are functions of k_x. However, Eq. (5) shows that ε_{yy} is equal to the arithmetic mean permittivity in the grating region, which is much larger in value than the mean harmonic permittivity ε_{xx}, for highly conducting lamellae. By taking this into account, the characteristic equation is drastically simplified:

$$\alpha = ik_{y,2}\, \mathrm{tg}(k_2h)/\varepsilon_{xx}, \qquad k_{y,2} \approx k_0\sqrt{\varepsilon_{xx}\mu_{zz}}\,. \qquad (15)$$